Absorption modification by laser irradiation in DKDP crystals

Xiaocong Peng (彭小聪)[1,2], Yuanan Zhao (赵元安)[1,3,*], Yueliang Wang (王岳亮)[1,2,4], Guohang Hu (胡国行)[1], Liujiang Yang (杨留江)[1], and Jianda Shao (邵建达)[1]

[1]*Key Laboratory of Materials for High Power Laser, Shanghai Institute of Optics and Fine Mechanics, Chinese Academy of Sciences, Shanghai 201800, China*

[2]*University of Chinese Academy of Sciences, Beijing 100049, China*

[3]*State Key Laboratory of Applied Optics, Changchun Institute of Optics, Fine Mechanics and Physics, Chinese Academy of Sciences, Changchun 130033, China*

[4]*National Engineering Laboratory for Modern Materials Surface Engineering Technology, Guangdong Institute of New Materials, Guangzhou 510650, China*

**Corresponding author: yazhao@siom.ac.cn*

Received January 23, 2018; accepted March 23, 2018; posted online April 24, 2018

Laser-induced modification at 355 nm of deuterated potassium dihydrogen phosphate (DKDP) crystals following exposure to nanosecond (ns) and sub-ns laser irradiation is investigated in order to probe the absorption mechanism in damage initiation. Laser damage resistance is greatly improved by sub-ns laser conditioning, whereas only a little improvement occurred after ns laser conditioning at the same laser fluence. Moreover, scattering and transmittance variations after the two types of laser conditioning indicate similar reduction of linear absorption. However, by contrast, large differences on nonlinear absorption modification are discovered using Z-scan measurement. This characteristic absorption modification by laser irradiation provides evidence that a nonlinear absorption mechanism plays a key role in damage initiation at 355 nm.

OCIS codes: 160.4670, 190.4180, 160.4760.
doi: 10.3788/COL201816.051601.

The effort to understand the underlying physical process involved in damage initiation in potassium dihydrogen phosphate (KDP) and its deuterated analog (DKDP) for large-aperture, high-power laser systems has lasted for more than half a century[1–5]. A localized absorption of laser energy by absorbing defects (called as precursors) is widely recognized as a major reason for laser-induced damage (LID)[5–8]. However, the absorption mechanism for damage initiation is not consistent. Several studies showed that macroscopic absorption depends linearly on the pump beam fluence, and absorption decreased after laser irradiation; whereas, they also observed a weak correlation between linear absorption and the LID in crystals[6,9]. On the other hand, Carr *et al.* observed sharp steps in the damage threshold of DKDP crystal and proposed a defect assisted multistep/photon absorption in crystals[10]. Preliminary models proposed that extrinsic defects, such as impurities and inclusions, act as gray bodies, absorbing a fraction of incident radiation linearly[7,11,12]. More recently, Liao *et al.* developed a self-consistent empirical model to predict the damage behavior after laser irradiation by assuming including two populations of absorbing defects, one with linear absorption and another with nonlinear absorption[13,14]. However, few literatures have been reported on the nonlinear absorption modification in DKDP crystals. Our previous works revealed that a kind of absorption defects existed, and linear absorption could be mitigated by laser conditioning[15,16]. More investigations are required to confirm the nonlinear absorption modification in DKDP crystals.

In this Letter, laser-induced modification at 355 nm by nanosecond (ns) and sub-ns lasers is studied. Specifically, laser damage performance of pristine (prior to irradiation) and laser conditioned DKDP crystals are compared. Scattering and transmittance variations by laser conditioning are observed with low energy light illumination. Moreover, a single beam Z-scan technique is used to investigate the nonlinear absorption variation. The objective of this work is to provide insight into the nonlinear absorption affecting the ns laser damage performance. The DKDP samples used in this study were 70% deuterated and cut in a Type II third harmonic generation (THG) orientation from conventionally grown DKDP boules to 50 mm × 50 mm × 10 mm size plates and polished to optical quality on all sides. Moreover, the samples used in the Z-scan measurement were thinned to about 5 mm to make them suitable for testing.

The samples were pre-exposed using two laser sources, all operating at 355 nm but with different pulse lengths and beam sizes. One was a tripled laser using a master-oscillator power amplifier (MOPA) operating at 10 Hz with a pulse duration of approximately 0.85 ns (full width at half-maximum, FWHM) labeled sub-ns laser, and the other was a commercial tripled neodymium-doped yttrium aluminum garnet (Nd:YAG) laser operating at 10 Hz with about 7.6 ns (FWHM) Gaussian pulses labeled ns laser. The diameter (1/e) of the sub-ns laser spot on the samples

was about 0.39 mm. A raster scan was performed at a fluence of 1 J/cm^2. The distance between the centers of the nearby beam spots was set at 0.10 mm, which was determined from the 90%-of-peak-fluence beam diameter to ensure that each space over the entire crystal bulk can be uniformly irradiated at high energy. The ns laser had a 1/e full width of about 0.90 mm on the samples. A raster scan was also performed at a fluence of 1 J/cm^2, and the distance between the centers of the nearby beam spots was set at 0.25 mm. Therefore, three kinds (pristine, ns laser conditioned, and sub-ns laser conditioned) of samples were prepared.

The damage testing at 355 nm was performed using the ns laser. The damage sites were illuminated with a He–Ne laser, which was collinear with the damage beam, and the image of the bulk damage region was captured orthogonally to the direction of laser propagation by a CCD camera through the side of the sample. The LID thresholds (LIDTs) were measured using a one-on-one testing procedure. The LIDT was defined as the maximum fluence without damage occurring, and 10 sites were tested. The total error of the damage probability was about 15%.

The scattering and transmittance variation by laser pre -exposed (or conditioning) were measured by the systems described in detail in Ref. [15]. The variation in scattering was obtained by comparing the images captured before and after laser irradiation. In the transmittance measurement, a 355 nm continuous-wavelength laser was split into a detection beam and a reference beam, and the power of the detection beam was approximately 1 mW.

The nonlinear optical properties of the pristine and laser conditioned samples were investigated using an open-aperture Z-scan system[17–19]. Total transmittance through the samples as a function of the incident intensity was measured, while the samples were gradually moved through the focus of a lens along the z axis. All experiments were performed using 340 fs pulses from a mode-locked fiber laser at 515 nm (2.41 eV) with the repetition rate of 1 kHz. The laser beam was tightly focused through a lens with a focal length of 15 cm. The laser beam waist radius at the focus was estimated to be ~18.5 μm, and the pulse energy reaching the sample was ~400 nJ.

The results of the one-on-one damage tests at 355 nm on three kinds of samples are shown in Fig. 1. Overall, the damage probability curve of the sub-ns laser conditioned material shifts noticeably to higher fluence, and only small improvements occur after ns laser conditioning compared to that of the pristine material. Moreover, the LIDT of the pristine and ns laser conditioned material is ~4.0 J/cm^2, whereas it is ~6.4 J/cm^2 in the sub-ns laser conditioned sample, which is a 1.6 times improvement in the LIDT after sub-ns laser conditioning. Therefore, it can be concluded that laser conditioning with sub-ns pulses can dramatically improve damage resistance, even if the conditioning fluence was as low as 1 J/cm^2.

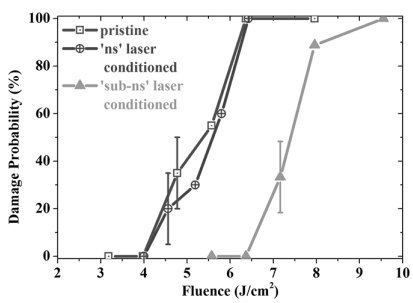

Fig. 1. One-on-one damage probability curves of three kinds of samples.

These results indicate that the distribution of precursor defects in crystals is modified via the laser conditioning process. As shown in Table 1, most of scattering defects disappeared after ns and sub-ns laser conditioning in these samples. Moreover, the transmittance increases about 4.23×10^{-3} after sub-ns laser conditioning. As mentioned in Ref. [15], relative to absorption, scattering has a very low contribution in transmittance variation; therefore, the transmittance increase is mainly due to the decrease in absorption. Furthermore, the power of the detection laser is so low that the decrease in absorption is referred to as a linear absorption property. Thus, the decrease in absorption by sub-ns laser conditioning is about 4.23×10^{-3}, and it seems that the linear absorption decrease could be the reason for the noteworthy improvement in the laser damage resistance after sub-ns laser conditioning. However, a transmittance increase of about 4.38×10^{-3} and only a small improvement in the laser damage resistance after ns laser conditioning (shown in Fig. 1) are also observed. These results imply that another type of absorption, such as nonlinear absorption mentioned in Refs. [10,14], is more likely to contribute to the enhancement in the laser damage resistance.

To gain more insight into the laser-induced modification of the laser–matter interactions, we performed open-aperture Z-scan measurements on these three series of samples with the intention of calculating their nonlinear absorption coefficients. The curve exhibits a normalized transmittance valley, indicating the occurrence of induced absorption in the samples, as shown in Fig. 2. The nonlinear transmittance of pristine, ns laser, and sub-ns laser conditioned materials at peak intensity were ~70.5%, ~71.3%, and ~77.6%, respectively. It indicated that nonlinear absorption was reduced by sub-ns laser conditioning.

Table 1. Transmittance Increase and Scattering Defects Decrease by Two Types of Laser Conditioning Procedures

Procedure	Scattering Decrease (%)	Transmittance Increase (%)
Sub-ns laser conditioning	86.25	0.423
ns laser conditioning	81.91	0.438

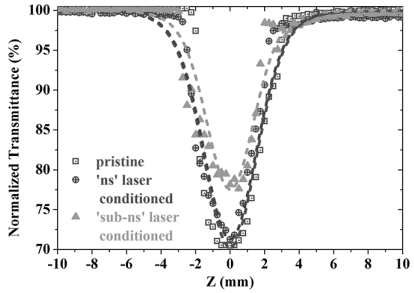

Fig. 2. Typical Z-scan curves for three kinds of samples. The dotted lines represent the theoretical fitting. The dots represent experimental data.

The photon energy of the excitation laser is ∼2.41 eV, and the band gap value of DKDP crystals is estimated to be close to 7.8 eV (>3 × 2.41 eV)[3,5,10]. Thus, the obtained nonlinear behaviors are numerically confirmed to be due to four-photon absorption (4PA) by fitting the data to the appropriate nonlinear transmission equation[20,21],

$$T_{4\mathrm{PA}}(z) = \frac{\int_{-\infty}^{\infty}\int_{0}^{\infty} 2\pi \frac{I(r,z,t)\exp(-\alpha_0 L)(1-R)}{[1+3\gamma L_{\mathrm{eff}} I^3(r,z,t)]^{1/3}}\, r\mathrm{d}r\mathrm{d}t}{\exp(-\alpha_0 L)(1-R)\int_{-\infty}^{\infty}\int_{0}^{\infty} 2\pi I(r,z,t) r\mathrm{d}r\mathrm{d}t}, \quad (1)$$

where the intensity in the samples is written as

$$I(r,z,t) = \frac{I_0(1-R)\exp(-t^2)}{1+z^2/z_0^2}\ \exp\left[\frac{-2r^2}{\omega_0^2(1+z^2/z_0^2)}\right], \quad (2)$$

where I_0 is the on-axis peak intensity at the focus; z is the sample position with respect to the focal point of the focused beam; ω_0, λ, and $z_0 = \pi\omega_0^2/\lambda$ are the waist radius, wavelength, and the diffraction length of the Gaussian beam, respectively. R is the surface reflectivity, γ is the effective 4PA coefficient, α_0 is the linear absorption coefficient, and $L_{\mathrm{eff}} = [1-\exp(-3\alpha_0 L)]/(3\alpha_0)$ is the samples' effective thickness. The best fit values (γ) with a coefficient of determination of above 0.96 are shown in Table 2.

Furthermore, absorption is usually quantified by an absorption cross-section σ, which has units of area. The 4PA cross-section (σ_4) of the materials was calculated by $\sigma_4 = [(h\upsilon)^3\gamma]/N_0$; where $h\upsilon$ is the incident photon energy (2.41 eV), and N_0 is the concentration of absorbing species/centimeter cubed (cm^3). The density of valence electrons induced by point defects is assumed to be 5×10^{19} cm^{-3}[3,5]. The 4PA cross-section of the pristine material is about $(5.62 \pm 1.14) \times 10^{-108}$ $\mathrm{cm}^8 \cdot \mathrm{s}^3$. The obtained 4PA cross-section is far larger than the representative value in wide band gap ideal materials, which is on the order of 1×10^{-114} $\mathrm{cm}^8 \cdot \mathrm{s}^3$[10]. It confirms that the crystal is not ideal material, and intra-band defect states are present in crystals. Moreover, the value of nonlinear absorption coefficient reduces a little after ns laser conditioning, while almost halves to $(2.53 \pm 0.98) \times 10^{-6}$ $\mathrm{cm}^5/\mathrm{GW}^3$ after sub-ns laser conditioning. These results reveal that the nonlinear absorption is remarkably mitigated by sub-ns laser conditioning at 355 nm.

Table 2. 4PA Coefficients of the Three Types of Samples

Sample	γ (10^{-6} $\mathrm{cm}^5/\mathrm{GW}^3$)
Pristine	4.90 ± 0.99
ns laser conditioned	4.81 ± 1.37
Sub-ns laser conditioned	2.53 ± 0.98

Owing to significant advancements in the growth quality, some kinds of defect structures created (rather than foreign particles incorporated) during growth have been postulated to be the key ingredients that make up the precursor[3,5,22]. The key feature of the crystal structure of DKDP is covalently bonded molecular PO_4 units linked by a network of relatively weak hydrogen O–H(D)–O bonds. The defects formed are essentially connected with the proton transport within the hydrogen bond network[23,24]. The existence of various atomic defects is also identified with electron paramagnetic resonance (EPR) spectroscopy[5,10]. Moreover, density functional theory calculations have demonstrated that defects of some species create one state in the band gap of crystals, such as interstitial hydrogen in its neutral state, leading to electronic states in the band gap that can be associated with absorption at low photon energies, whereas some can provide two states[5,24–26]. Some experimental results are obtained with the pump probe method, which is always used in investigating the relaxation dynamics of materials[23,27–30], also suggesting the presence of defect states located in the band gap[23,29]. Thus, clusters of atomic intrinsic defects, such as hydrogen or oxygen atoms as interstitial atoms or vacancies, could be responsible for the linear and/or nonlinear absorption mechanism in crystals; absorption modification by laser irradiation is associated with alterations in the defect properties[5,11,15,22,31,32].

Within the long-accepted linear absorption model, laser conditioning is proposed to take place with a significant temperature rise because of heating effects. On one hand, this may result in a phase transition in the vicinity of the precursor defect, and subsequent rearrangements of the crystalline lattice that remove the defect and absorption efficiency vanishes during the cooling process[7,11]. On the other hand, this could bring about thermally activated migration and decreases in absorption by decreasing the number of absorbing defects through a recombination process during their migration[7]. However, our laser damage testing results have suggested that linear absorption is not the main mechanism responsible for damage initiation at 355 nm, which is in agreement with previous reports[5,22,33].

There is a possible explanation for this phenomenon. Besides the heating process for conditioning of precursors, the other pathway is an electronic process. There are great differences in the formation energy among different electronic defects[26]. In addition, not all of these defects are stable at room temperature[5]. The appearance probability

of the clusters of defects responsible for linear absorption may be far lower than that related to nonlinear absorption at room temperature.

In the case of multi-photon ionization assisted by defect states, states located in the band gap can offer a ladder for ground state electrons to make a transition to the conduction band and enhance electron transition probabilities to result in premature breakdown and damage[34]. These imply that a defect assisted multi-photon process works in the abovementioned 4PA process at 515 nm. Furthermore, the atomic defect clusters, which induce states in the band gap, may be unstable due to over absorption of the laser energy[9]. The breaking apart of defect clusters via sub-damage threshold laser irradiation is positively related to incident intensity. The laser intensity of the sub-ns laser is about eight times larger than that of the ns laser at a fluence of 1 J/cm^2. Thus, sub-ns laser irradiation is more effective in breaking defect clusters. The density of defect clusters relating to intra-band states can be significantly reduced by sub-ns laser pre-exposing. Therefore, the nonlinear absorption coefficient can be smaller by sub-ns laser conditioning at 355 nm, as shown in Table 2. Besides that, the precursor defects require a higher ns laser energy density to induce damage after laser irradiation at 355 nm (shown in Fig. 1). Therefore, the nonlinear absorption plays a key role in laser damage initiation, and the nonlinear absorption could be reduced by laser irradiation.

In conclusion, laser-induced modification at 355 nm in DKDP crystals was present in this Letter. The laser damage resistance of crystals was greatly improved by sub-ns laser conditioning. Furthermore, corresponding absorption (both linear and nonlinear) modification by laser irradiation was also demonstrated. It was proposed that, relative to linear absorption, the nonlinear absorption may play a key role in laser damage initiation. This study can provide additional insight in understanding absorption mechanisms in damage initiation.

This work was supported by the National Natural Science Foundation of China (Nos. 61405219 and 11304328).

References

1. A. Savage and R. C. Miller, Appl. Opt. **1**, 661 (1962).
2. P. A. Baisden, L. J. Atherton, R. A. Hawley, T. A. Land, J. A. Menapace, P. E. Miller, M. J. Runkel, M. L. Spaeth, C. J. Stolz, T. I. Suratwala, P. J. Wegner, and L. L. Wong, Fusion Sci. Technol. **69**, 295 (2016).
3. G. Duchateau, M. D. Feit, and S. G. Demos, J. Appl. Phys. **115**, 103506 (2014).
4. Y. Zheng, L. Ding, X. Zhou, R. Ba, J. Yuan, H. Xu, X. Yang, B. Chen, J. Na, Y. Li, and W. Zheng, Chin. Opt. Lett. **14**, 051601 (2016).
5. S. G. Demos, P. DeMange, R. A. Negres, and M. D. Feit, Opt. Express **18**, 13788 (2010).
6. M. Pommiès, D. Damiani, B. Bertussi, J. Capoulade, H. Piombini, J. Y. Natoli, and H. Mathis, Opt. Commun. **267**, 154 (2006).
7. G. Duchateau, Opt. Express **17**, 10434 (2009).
8. J. Chang, Y. Zhao, G. Hu, Y. Wang, D. Li, X. Liu, and J. Shao, Chin. Opt. Lett. **13**, 081601 (2015).
9. S. G. Demos, M. Staggs, and H. B. Radousky, Phys. Rev. B **67**, 224102 (2003).
10. C. W. Carr, H. B. Radousky, and S. G. Demos, Phys. Rev. Lett. **91**, 127402 (2003).
11. M. D. Feit, A. M. Rubenchik, and A. H. Guenther, Proc. SPIE **5273**, 74 (2004).
12. G. Duchateau and A. Dyan, Opt. Express **15**, 4557 (2007).
13. Z. M. Liao, M. L. Spaeth, K. Manes, J. J. Adams, and C. W. Carr, Opt. Lett. **35**, 2538 (2010).
14. Z. M. Liao, R. Roussell, J. J. Adams, M. Runkel, W. T. Frenk, J. Luken, and C. W. Carr, Opt. Mater. Express **2**, 1612 (2012).
15. Y. Wang, Y. Zhao, G. Hu, X. Peng, J. Chang, X. Xie, J. He, M. Guo, and J. Shao, Opt. Express **23**, 16273 (2015).
16. G. Hu, Y. Zhao, D. Li, and Q. Xiao, Opt. Express **20**, 25169 (2012).
17. M. Sheikbahae, A. A. Said, T. H. Wei, D. J. Hagan, and E. W. Vanstryland, IEEE J. Quantum Electron. **26**, 760 (1990).
18. J. Z. Li, H. X. Dong, B. Xu, S. F. Zhang, Z. P. Cai, J. Wang, and L. Zhang, Photon. Res. **5**, 457 (2017).
19. S. F. Zhang, Y. X. Li, X. Y. Zhang, N. N. Dong, K. P. Wang, D. M. Hanlon, J. N. Coleman, L. Zhang, and J. Wang, Nanoscale **8**, 17374 (2016).
20. R. L. Sutherland, *Handbook of Nonlinear Optics* (CRC Press, 2003).
21. B. Gu, X. Q. Huang, S. Q. Tan, M. Wang, and W. Ji, Appl. Phys. B **95**, 375 (2009).
22. P. DeMange, C. W. Carr, R. A. Negres, H. B. Radousky, and S. G. Demos, J. Appl. Phys. **104**, 103103 (2008).
23. G. Duchateau, G. Geoffroy, A. Dyan, H. Piombini, and S. Guizard, Phys. Rev. B **83**, 075114 (2011).
24. C. S. Liu, N. Kioussis, S. G. Demos, and H. B. Radousky, Phys. Rev. Lett. **91**, 015505 (2003).
25. C. S. Liu, C. J. Hou, N. Kioussis, S. G. Demos, and H. B. Radousky, Phys. Rev. B **72**, 134110 (2005).
26. K. P. Wang, C. S. Fang, J. X. Zhang, C. S. Liu, R. I. Boughton, S. L. Wang, and X. Zhao, Phys. Rev. B **72**, 184105 (2005).
27. K. Wei, X. Zheng, X. A. Cheng, C. Shen, and T. Jiang, Adv. Optical Mater. **4**, 1993 (2016).
28. C. Shen, M. Chambonneau, X. A. Cheng, Z. J. Xu, and T. Jiang, Appl. Phys. Lett. **107**, 111101 (2015).
29. C. D. Marshall, S. A. Payne, M. A. Henesian, J. A. Speth, and H. T. Powell, J. Opt. Soc. Am. B **11**, 774 (1994).
30. Y. Zhang, Q. Z. Zhao, H. H. Pan, C. W. Wang, J. Qian, and Z. S. Wang, Chin. Opt. Lett. **14**, 083201 (2016).
31. S. G. Demos, M. Yan, M. Staggs, J. J. De Yoreo, and H. B. Radousky, Appl. Phys. Lett. **72**, 2367 (1998).
32. M. M. Chirila, N. Y. Garces, L. E. Halliburton, S. G. Demos, T. A. Land, and H. B. Radousky, J. Appl. Phys. **94**, 6456 (2003).
33. P. DeMange, R. A. Negres, A. M. Rubenchik, H. B. Radousky, M. D. Feit, and S. G. Demos, J. Appl. Phys. **103**, 083122 (2008).
34. G. Duchateau, M. D. Feit, and S. G. Demos, J. Appl. Phys. **111**, 093106 (2012).